PH SHIFTS IN TRIS BUFFER DURING FREEZE THAWING

A THESIS

SUBMITTED TO THE FACULTY OF THE GRADUATE SCHOOL

OF THE UNIVERSITY OF MINNESOTA

BY

WENQI GAI

IN PARTIAL FULFILLMENT OF THE REQUIREMENTS

FOR THE DEGREE OF

MASTER OF SCIENCE

PROFESSOR. RAJ SURYANARAYANAN

JUNE 2023

ACKNOWLEDGEMENT

First, I would like to thank my advisor Dr. Raj Suryanarayanan for his guidance and financial support during my graduate study. His dedication to solid-state pharmaceutical research motivates me to conquer difficulties and solve problems. To me, he is not only an excellent mentor, but also a patient grandfather.

Besides, I would like to thank my dissertation committee, Drs. Ronald A. Siegel and Christopher J. Douglas, for their input and valuable suggestions for my thesis.

I want to especially thank Dr. Ronald A. Siegel for providing me with a valuable opportunity in his lab to start pharmaceutical research during my undergraduate study.

I am also very grateful to Jinghan Li for his valuable contribution and support when developing this research project. In addition, I appreciate all the generous help from Dr. Dominik Heger from Masaryk University on low temperature pH measurements using cresol red (CR) and data interpretation. I would also like to thank Dr. Robert Schumacher from the Center for Translational Medicine, University of Minnesota for providing partial financial support.

I would also like to thank other Sury lab members, Drs. Jayesh Sonje, Bhushan Munjal, N. S. Krishna Kumar, and Rahul Lalge for their encouragement and support in my graduate study. I would also express my appreciation to the Department of Pharmaceutics, especially, Katie, Jody, and Amanda for all the support.

Finally, I would like to thank my family and friends for their support.

DEDICATION

For my parents, Xiuyu Sun and Ming Gai.

ABSTRACT

Purpose: To study the phase behavior of tris buffer during freeze and thawing and monitor the resulting pH changes.

Methods: Tris buffer, at concentrations of 10 mM and 100 mM, and room temperature pH values (pH_0) of 7.3, 8.0 and 8.8 are studied. The phase behavior of tris buffers under subambient conditions was characterized by thermal (differential scanning calorimetry, DSC), spectroscopic (UV-Vis spectrophotometer) and X-ray diffractometric (synchrotron X-ray diffractometry, SXRD) techniques. Cresol red (CR) was added as the pH indicator to measure the pH of frozen tris solutions.

Results: According to the DSC results, (i) both tris base and tris HCl crystallized during freeze thawing. (ii) Compared with tris base, tris HCl exhibited a higher crystallization propensity. (iii) The crystallization of tris HCl was more pronounced at higher solute concentrations. (iv) As the concentration of tris base increased (i.e., higher pH), there was more pronounced inhibition of tris HCl crystallization. In other words, tris base exhibited a concentration dependent inhibition of tris HCl crystallization. SXRD results confirmed that at subambient conditions, tris HCl has a substantially higher crystallization propensity than tris base. Its crystallization was often observed during heating. In the current study of buffers with pH_0 7.3, 7.5, and 7.9, the increase in Hammett Acidity function (H_x) is ~ 0.3 to 0.4 unit per 10 °C decrease, possibly indicating that the positive pH shift of tris buffer at subambient conditions is attributable to increasing pK_a rather than tris HCl crystallization.

Conclusion: Tris base exhibited a concentration dependent inhibition of tris HCl crystallization. The positive pH shift of tris buffer at subambient conditions is attributable to increasing pK_a rather than tris HCl crystallization.

Keywords

tris buffer, phase behavior, pH, freeze thawing, differential scanning calorimetry, UV-Vis spectroscopy, pH indicator dye, cresol red, Synchrotron X-ray diffractometry

TABLE OF CONTENTS

LIST OF TABLES

LIST OF FIGURES

LIST OF ABBREVIATIONS

tris base: Tris(hydroxymethyl)aminomethane

tris HCl: Tris(hydroxymethyl)aminomethane hydrochloride

tris buffer: Tris(hydroxymethyl)aminomethane-hydrochloride buffer

CR: Cresol red

UV-Vis spectroscopy: Ultraviolet–visible spectroscopy

DSC: Differential scanning calorimetry

SXRD: Synchrotron X-ray diffractometry

T_g': Glass transition temperature of the freeze-concentrate

T_c: Crystallization onset temperature

RT: Room temperature

pH_0: Initial pH value at room temperature

H_x: Hammett acidity function

INTRODUCTION

Tris(hydroxymethyl)aminomethane (tris)-hydrochloride (HCl) buffer system

A variety of diseases including cancers and chronic conditions such as arthritis, asthma and psoriasis are treated with protein pharmaceuticals [1]. Proteins, before they are formulated into dosage forms, are often stored as solutions. The solutions are often buffered and may also contain sodium chloride and other solutes. Histidine, phosphate, citrate, tris, and succinate buffers are the most commonly used buffer systems in protein formulations [2].

Protein solutions, in light of their degradation propensity, are often transported as well as stored in the frozen state.[3] However, when frozen, because of ice crystallization, there will be a pronounced increase in the solute concentration as well as the ionic strength in freeze-concentrate. There is also the possibility of selective crystallization of a buffer component leading to alteration in solution pH values. All these factors can lead to the destabilization of the drug substance [3, 4].

In this study, we will focus on the tris(hydroxymethyl)aminomethane (tris base) and tris(hydroxymethyl)aminomethane hydrochloride (tris HCl) buffer system. Tris buffer is widely used in numerous biopharmaceutical products, such as YERVOY® (ipilimumab, Bristol-Mysers Squibb) and LEUKINE® (Sargramostim, Sanofi) [5 - 7]. It is also used in the novel mRNA COVID-19 vaccine developed by Pfizer/BioNTech and Moderna [8].

Tris base is a weak base (B) and its ionization is brought about by its acceptance of a proton to form the conjugate cation acid (BH^+) (**Equation 1; Figure 1).** The equilibrium constant (also referred to as acid dissociation constant, K_a) is expressed in **Equation 2**.

$$BH^+ + H_2O \quad \rightleftharpoons \quad B + H_3O^+ \qquad (1a)$$

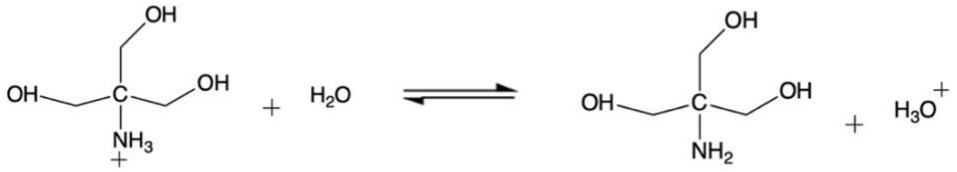

(1b)

Figure 1. Ionization behavior of tris(hydroxymethyl)aminomethane hydrochloride in aqueous solution. The pK_a value of tris(hydroxymethyl)aminomethane hydrochloride is 8.1 at 25 °C [9].

$$K_a = \frac{[H^+][B]}{[BH^+]} \qquad (2)$$

Based on the pK_a and ratio of tris base (B) to tris HCl (BH^+), the pH value of the buffer solution can be calculated using the Henderson-Hasselbalch equation (**Equation 3**).

$$pH = pK_a + \log\frac{[B]}{[BH^+]} \qquad (3)$$

Tris buffer is chemically stable and compatible with most proteins and other biomolecules. It is suitable to buffer solutions over the pH range of 7 ~ 9 which is ± 1 unit of the acid dissociation constant (pK_a) of the buffer (**Figure 1**) [10].

Although tris buffer is chemically stable, its pK_a is highly temperature dependent, when solutions buffered with tris are cooled, there is a potential for pH shift. This effect can induce product destabilization during processing where the drug substance undergoes substantial changes in temperature (e.g., freezing and freeze drying). Considering buffer salts with amino groups (e.g., tris), their pK_a were sensitive to temperature and elevated as the temperature decreases [11]. The K_a of a buffer system, as a function of temperature, is explained by the extended van't Hoff equation (**Equation 4**).

$$\ln K_2 = \frac{\Delta H_1 - T_1\Delta Cp_1}{R}\left(\frac{1}{T_1} - \frac{1}{T_2}\right) + \frac{\Delta Cp_1}{R}\ln\left(\frac{T_2}{T_1}\right) + \ln K_1 \qquad (4)$$

where K_1 and K_2 are the acidic dissociation constants at temperatures T_1 and T_2, respectively, ΔCp_1 is the heat capacity change at T_1, ΔH_1 is the change of enthalpy of ionization at T_1, and R is the ideal gas constant. It is assumed that ΔCp_1 and ΔH_1 are temperature independent.

Based on the ΔCp_1 of -59 J/(K·mol) and ΔH_1 of 47.45 kJ/mol (at T_1, or 25 °C) from Goldberg et al., the acidic dissociation value of tris buffer is highly temperature dependent, resulting in ~ 0.41 units of pK_a increase as temperature decreases every 10 °C [10]. Kolhe et al. reported that a 20 mM tris solution exhibited 0.22 unit increase in pH for every 10 °C decrease in temperature [12]. There is a difference between the calculated pK_a value based on the extended van't Hoff equation and the experimental pH values, the degree of ionization of tris is more sensitive to temperature than many other compounds [11].

When the buffer solution is cooled, selective crystallization of a buffer component can cause a pronounced pH shift and induce protein denaturation. For example, during freezing, the crystallization of disodium phosphate dodecahydrate resulted in up to 4 units of reduction in pH and induced aggregation of bovine serum albumin and β-galactosidase [13]. In tris buffer, both tris base and tris HCl could crystallize at subambient conditions, as evident from crystallization at -27 and -39 °C and eutectic melting at -6 and -13 °C of the base and salt, respectively [14]. Although tris buffer did not exhibit a substantial pH shift upon freezing, such a conclusion was based on pH measurement up to -30 °C [12]. It was not possible to evaluate the effect of tris buffer salt crystallization on solution pH at lower temperatures - 30 °C . For example, during the freezing stage of lyophilization (up to -50 °C) and frozen storage (up to -80 °C). Thus, we wish to comprehensively characterize the phase behavior of frozen tris buffer, and study the effect of buffer salt crystallization, if any, on solution pH value.

pH indicator dye: Cresol Red

Since the crystallization of tris base and tris HCl was observed at -27 and -39 °C, respectively, the low temperature pH probe was deemed unsuitable for the comprehensive study of pH shift induced by buffer salt crystallization [14]. Thus, to understand the impact of tris buffer salt crystallization on solution pH, cresol red (CR), a pH sensitive indicator dye (**Figure 2.**), was used to measure the "pH" of frozen tris buffer solutions. CR belongs to the class of 2,1-benzoxathioles and both hydrogens at position 3 are substituted by 4-hydroxy-5-methylphenyl groups [15]. CR can be used to determine pH at the ranges of ~ 0 to 3.1 and ~ 6.2 to 10.2, which are ± 2 units of the pK_a of the indicator dye (pK_a^1 = 1.1 and pK_a^2 = 8.2) [16]. It can be used in the pH (or acidity) measurement of liquid, frozen and solid samples [16]. The three forms of CR in aqueous solutions, all have zwitterionic structures with conjugation systems that exhibit different UV-Vis maximum absorbance wavelengths (λ_{max}) are shown in (**Figure 2)** [17]. To make the discussion easier, the three forms of CR at 518, 434 and 573 nm are referred to as H_2CR (doubly protonated), $H(CR)^-$ (singly protonated) and $(CR)^{2-}$ (deprotonated) (**Figure 2**). Since the pK_a^2 of CR (8.2) is close to the pK_a of tris base (8.1), it can be a desirable indicator dye to study any potential pH shift in the tris buffer solution. However, it should be noted that the pK_a^2 of CR is also temperature dependent [16]. However, the change in the pK_a^2 is not considered substantial. For example, it increases from 8.70 to 8.96 as the temperature reduces from -20 to -40 °C.

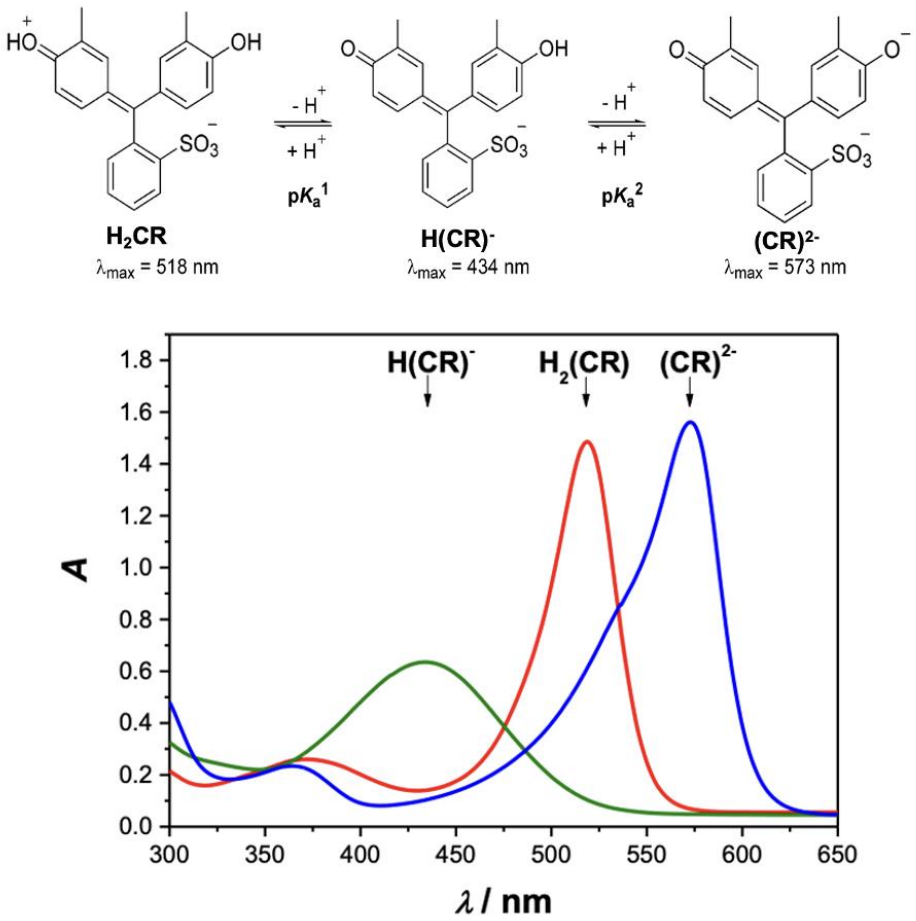

Figure 2. Structures of the three forms of CR in an aqueous solution (top) and absorbance (A) spectra of the three forms of CR in aqueous solution (bottom). H_2CR is a doubly protonated form of CR, $H(CR)^-$ is a singly protonated form of CR, and $(CR)^{2-}$ is a deprotonated form of CR [16, 17].

STRATEGIES AND HYPOTHESES

Based on our discussion in the previous section, we hypothesize that the change in the pK_a and the buffer salt crystallization could lead to pH shift in the frozen tris buffer solution. For this project, our working hypotheses are:

(i) In a buffer solution with an initial pH < pK_a, the conjugated acid (BH^+) was the predominant species. Upon cooling, the crystallization of the conjugated acid, in other words, tris HCl, would lead to an increase in pH. *Combined with the increased pK_a value at low temperatures, the crystallization of tris HCl is expected to induce a substantial elevation in pH*.

(ii) On the other hand, tris base (B) is the predominant species in the buffer solution at an initial pH > pK_a. *Upon cooling, tris base crystallization, if any, can result in a decrease in pH, which potentially counteracts the increase in pK_a at low temperatures. Thus, a substantial change in pH is not expected.*

(iii) For a buffer solution prepared at a pH close to its pK_a, the concentrations of the base and conjugate acid are approximately the same. Thus, in the frozen solution, the pH shift is dependent on the increased pK_a and the relative crystallization propensities of the tris base and tris HCl. *We hypothesize, that the increase in pK_a will be the dominant factor governing the increase in pH of the frozen solution*.

Although in the previous studies, pH shift in tris buffer at subambient conditions was not substantial, we aim to further understand the effect of buffer species (salt or acid) crystallization on the pH of the frozen solution, and its interplay with the change in pK_a as a function of temperature [13]. The phase behavior of frozen aqueous solution was characterized by differential

scanning calorimetry (DSC) and synchrotron X-ray diffractometry (SXRD). The indicator dye, cresol red was added to the buffer solution, and the pH was measured using UV-Vis spectroscopy.

MATERIALS AND METHODS

Materials

Tris base (MW 121.14 g/mol; assay ≥ 99.8 %; Fisher BioReagents™), tris HCl (MW 157.60 g/mol; ≥ 99 %; Sigma-Aldrich), hydrochloric acid (HCl) 36.5 - 38.0% (VWR International), and cresol red (CR; MW 382.43 g/mol; 96.5%; Chem-Impex International, Inc.) were obtained and used as received. Tris buffers at 10 mM and 100 mM concentrations were prepared by dissolving the required amount of tris base in water. Hydrochloric acid (100 mM) was used to titrate the solution until the desired pH value was reached. Solutions of 100 mM tris base (pH 10.5 at RT) and 100 mM tris HCl (pH 5.4 at RT) were also prepared.

CR (0.055 mg) was added to 100 mL of each tris solution to result in a final dye concentration of ~ 1.4×10^{-5} M.

Table 1. The composition of the tris buffer solutions.

pH Value*	Buffer concentration
7.3	10 to 300 mM
8.0	10 and 100 mM
8.8	10 and 100 mM

*pH measured at RT using Orion Star™ A211 Benchtop pH Meter, Thermo Scientific™.

Methods

Differential scanning calorimetry (DSC)

A differential scanning calorimeter (DSC) (Q2000, TA Instruments, New Castle, DE), with dry nitrogen gas purged at 50 mL/min, was used. A refrigerated cooling accessory was attached to the DSC. In the first set of studies, approximately 20 mg of solutions were weighed in an aluminum pan, sealed hermetically, equilibrated at 5 °C for 5 minutes, and then further cooled to -80 °C and equilibrated for 15 minutes. The frozen solutions were heated to 20 °C at 1 °C/min. In another set of studies, approximately 20 mg of solution were weighed in an aluminum pan, sealed hermetically, equilibrated at 5 °C for 5 minutes, cooled to -50 °C and equilibrated at -50 °C. for 15 minutes. The frozen solution was first heated to -20 °C at 1 °C/min and held isothermally for 8 hours and then heated to 20 °C at 1 °C/min. The crystallization onset temperature (T_c) is reported. The glass transition temperature (T_g) is reported at the transition midpoint.

Synchrotron X-ray diffractometry (SXRD)

The 17-BM-B (sector 17; Advanced Photon Source, Argonne National Laboratory, IL, USA) beamline was used. Sample solutions were first cooled from room temperature (RT) to -40 °C, held for 15 min, and then heated back to 5 °C at 2 °C/min. A monochromatic X-ray beam with wavelength (λ) of 0.45171 Å and beam size 300 μm x 300 μm, and a two-dimensional (2D) area detector (XRD-1621, Perkin Elmer) were used. A V-shaped sample holder taped with Kapton® was used to hold 100 μL of the sample solution and a Cryostream 700 plus system (Oxford Cryosystems Ltd, Oxford, UK) was used for cooling [18]. By using the sample holder without any solution, the background signal was obtained. A GSAS-II software (Edgewall Software) was used to convert the 2D X-ray patterns.

Low temperature pH measurement

The sample solution (3 mL) was placed in a glass UV cuvette and cooled using a benchtop freeze-dryer (VirTis AdVantage, Gardiner, NY). The solutions were first cooled from RT to −40 °C and heated to predetermined temperatures (-40, -30, and -20 °C). The heating and cooling rate was 1 °C /min. At -40, -30, and -20 °C, the frozen buffer solution was removed from the freeze-dryer and the absorbance was measured using a UV-Vis spectrophotometer (Cary 100 UV-Vis, Agilent Technologies).

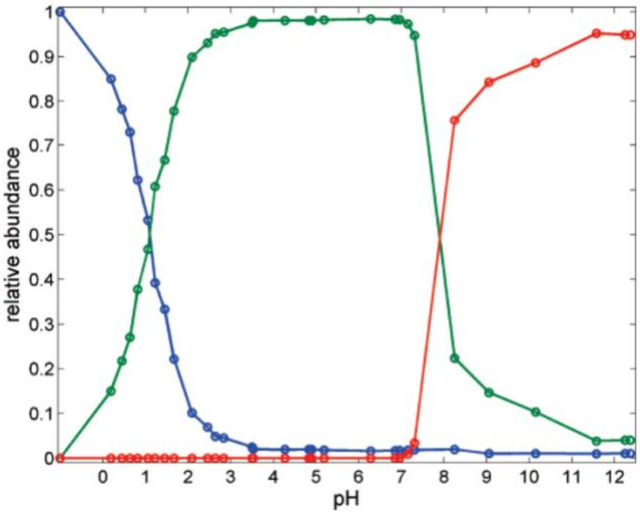

Figure 3. The calculated relative abundance profiles of three CR forms (H_2CR in blue, $H(CR)^-$ in green and $(CR)^{2-}$ in red) at room temperature as a function of pH [17].

The speciation of cresol red (CR) has been described by Heger et al (**Figure 3**) [17]. It is evident that at pH 4.5 and 11.5 at RT, the highest relative abundance of $H(CR)^-$ and $(CR)^{2-}$ respectively were observed (**Figure 3**) [17]. The aqueous CR red solutions of pH values 4.5 [$(H(CR)^-$] and 11.5 [$(CR)^{2-}$] at RT were obtained by titrating with 10 mM HCl or 10 mM NaOH, respectively. The use of the two reference indicator spectra, in the non-negative function of the linear least square regression (lsqnonneg function in MATLAB; **Script S9**), to calculate the pH values of the solutions is described below [16].

The UV-Vis spectra of the tris buffer solutions containing CR (1.4×10^{-5} M) in frozen state were collected in a spectrophotometer (Cary 100 UV-Vis, Agilent Technologies) directly after removal from freeze-dryer (LyoStar 3, SP Scientific, Warminster, PA). Likewise, the absorbance of the solutions was determined. The compositions of the systems studied are provided in **Table 1**.

In this context, it is instructive to introduce the Hammett acidity function (H_x), which is designed to measure the acidity of both dilute and concentrated solutions [19]. This is accomplished by studying the ionization of neutral acidic indicator molecules (**Equation 5**) [16]. The equation has been modified for the indicator of interest (cresol red) [16]:

$$H_x = pK_{a,\ CR} + \log\frac{C_{(CR)^{2-}}}{C_{H(CR)^{-}}} \qquad (5)$$

In the above equation, $C_{(CR)^{2-}}$ is the concentration of $(CR)^{2-}$, $C_{H(CR)^{-}}$ is the concentration of $H(CR)^{-}$, and $pK_{a,\ CR}$ is the acidity constant of the cresol red in dilute aqueous solution [16]. After CR is added to the solutions, in the pH range of 7 to 10, the singly pronated form $H(CR)^{-}$, and the deprotonated $(CR)^{2-}$ form could be observed in the spectrum. In dilute solutions, the activity coefficient is close to one, and pH equals to H_x [19].

The linear least square regression function (lsqnonneg function) was used to calculate the relative concentrations of $H(CR)^{-}$ (labeled as B) and $(CR)^{2-}$ (labeled as C) forms of the indicator labeled respectively as b and c in the equation. The sample spectrum is labeled as X. Using the values of b, c, and the corresponding pK_a of CR at the temperature, **Equation 6**, will provide the value of Hx [16].

$$\sum_{\lambda=400\ nm}^{650\ nm}(B\ b + C\ c - X)^2 = \min \qquad (6)$$

RESULTS AND DISCUSSION

DSC results

During the cooling of all the pure tris solutions, ice crystallized in the temperature range of -15 to -30 °C. While tris base solutions (both 500 and 100 mM) did not reveal solute crystallization (**Figure 4a**), the exotherm at ~ -30 °C observed in the tris HCl solution (broad peak) could be attributed to solute crystallization (**Figure 4b**). Upon heating the above frozen solutions, the 500 mM tris base solution showed a glass transition event at ~ -60 °C (**Figure 4c**). This is referred to as T_g', the glass transition temperature of the freeze-concentrate. This was lower than the reported value of -51 °C [14]. It must be pointed out that Chang et al. used a cooling rate of 200 °C/min and a heating rate of 10 °C /min [14]. The exotherm at -41 °C is attributable to the solute crystallization (tris base) and the accompanying unfrozen water. The endotherm at ~ -6 °C was the tris-water binary eutectic melting [14]. During heating of frozen tris HCl solution, no glass transition event was observed. This was not surprising since substantial solute crystallization was observed during cooling. In the 100 mM tris HCl solution, an exotherm was detected at -54 °C (**Figure 4d**), suggesting additional solute crystallization during heating. Finally, the eutectic melting of tris HCl-water binary mixture was observed at ~ -14 °C (**Figure 4d**). The measured eutectic melting temperatures of tris base and tris HCl are in excellent agreement with the reported values [14].

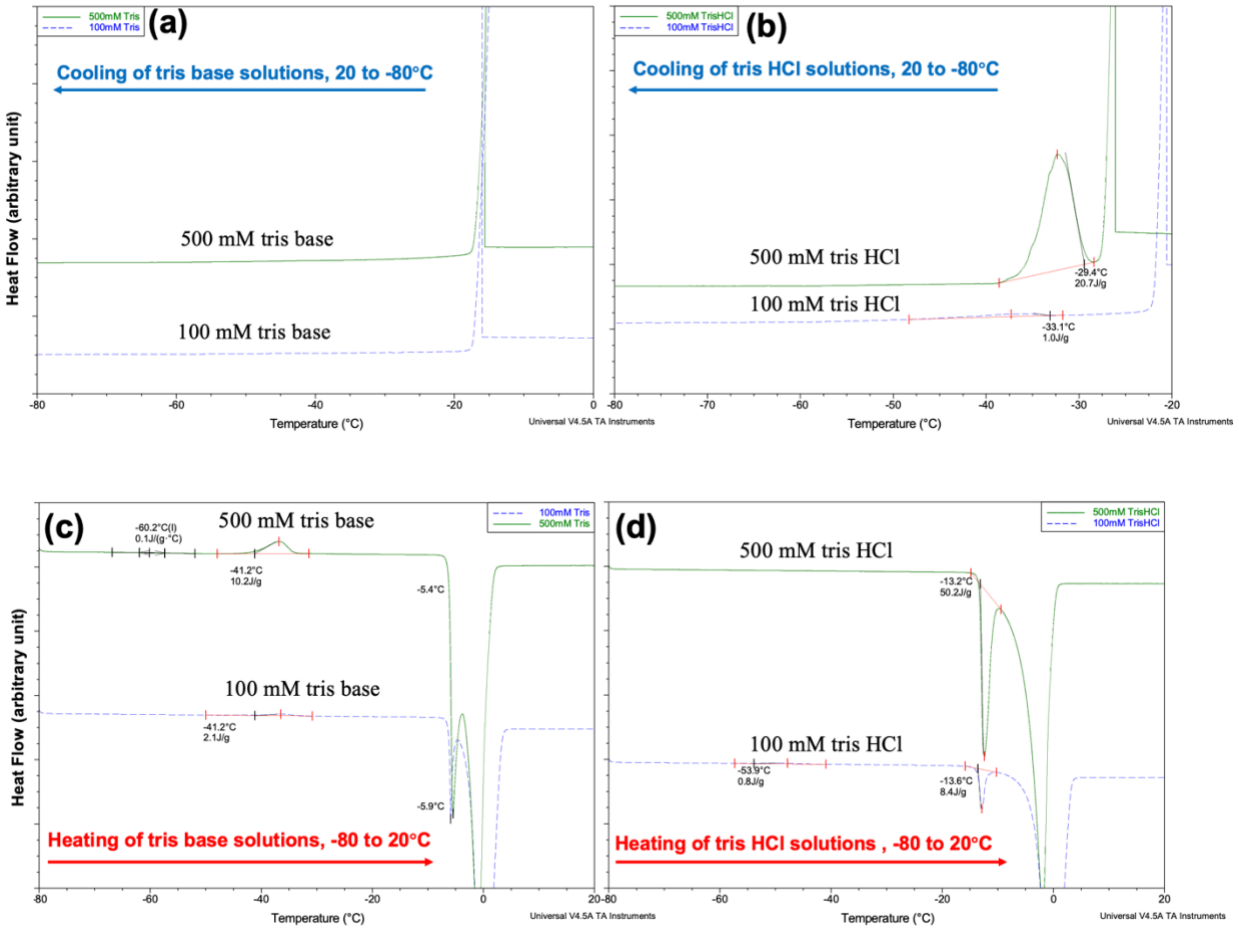

Figure 4. DSC cooling curves of aqueous solutions of (a) tris base and (b) tris HCl. The results of solute concentrations at 500 and 100 mM are shown in green and blue, respectively. The solutions were cooled from room temperature (RT) to -80 °C at 1 °C/min. The relevant heating curves of aqueous tris base and tris HCl solutions are shown in panels (c) and (d), respectively. The frozen solutions were heated from -80 to 20 °C at 1 °C/min.

For the tris solutions (both 10 and 100 mM) buffered to pH values of 7.3, 8.0 and 8.8 at RT, no solute crystallization was observed during cooling (**Figure S1**). During heating, neither solute crystallization nor eutectic melting was detected in the buffer solutions with initial pH values of 8.0 and 8.8. However, the 100 mM tris buffer solution with an initial pH of 7.3 revealed an exotherm at -49 °C followed by eutectic melting at ~ -15 °C (**Figure 5**). Since the tris HCl-ice eutectic temperature is -14 °C, the exotherm at -49 °C is attributed to the crystallization of tris HCl. Thus, in the 100 mM buffer solution (initial pH 7.3), the crystallization of tris HCl is observed not during cooling but during heating of the frozen solution. This is in contrast to the behavior of the

'as is' tris HCl solution (both 10 and 100 mM), wherein solute crystallization was observed during cooling (**Figure 4b**). When the buffer concentration was reduced to 10 mM (initial pH 7.3), there was no evidence of solute crystallization either during cooling or heating (**Figure 5**). However, solutions of both the concentrations (10 and 100 mM; initial pH 7.3), revealed eutectic melting at ~ -15 °C (**Figure 5**). Thus, we believe that at 10 mM buffer concentration, the solute crystallization is likely to have occurred over a wide temperature range, so it was not detectable by DSC. However, the eutectic melting endotherm is indirect evidence of solute crystallization. Notably, the eutectic melting temperatures observed in the buffer solutions were lower than that in pure tris HCl solution (-14 °C; **Figure 4d**).

The eutectic melting enthalpy of 100 mM tris HCl was 8.4 J/g (**Figure 4d**). For the sake of this discussion, we will assume the complete crystallization of tris HCl in the frozen solution. In the tris buffer of the same concentration (pH 7.3 at RT), the eutectic melting enthalpy was 5.2 J/g (**Figure 5b**). The pK_a of tris at -15 °C is calculated, using the extended van't Hoff equation, to be 9.4. At this temperature, the pH of tris buffer solution was determined to be 8.3 [12]. Using the Henderson-Hasselbalch equation, the fraction of tris HCl was calculated to be 0.92. If we again assume complete crystallization of tris HCl, the expected enthalpy value is 7.9 J/g. Since the observed melting enthalpy in the tris buffer solution (5.2 J/g) was lower than the calculated value (7.9 J/g), we speculate that the tris (base) inhibits the crystallization of tris HCl in frozen solutions.

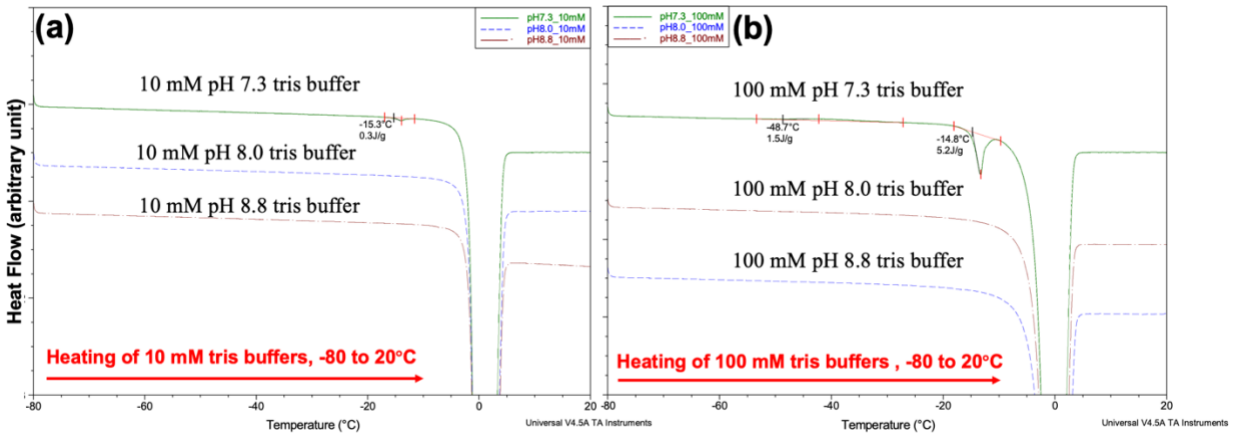

Figure 5. DSC heating curves of (a) 10 and (b) 100 mM tris buffer solutions. The pH values of the buffer solutions are pH 7.3* (green), 8.0* (blue) and 8.8* (brown). The solutions were initially cooled from room temperature to -80 °C, held for 15 minutes and then heated to 20 °C. Both the heating and cooling rates were 1°C/min. Only the final heating curve is shown. The DSC cooling curve is in the appendix (**Figure S1**). * pH measured at room temperature.

In order to investigate this further, 'as is' tris HCl and tris buffer (initial pH 7.3) solutions were prepared, over a concentration range of 10 to 300 mM, and the DSC results were compared (**Figure 6**). Tris buffer solutions (pH 7.3 at RT, over the concentration range of 10 to 300 mM) did not reveal solute crystallization upon cooling (**Figure 6a**). On the other hand, solute crystallization at ~ -30 °C was observed in the DSC cooling curves of pure tris HCl solution at concentrations ≥ 100 mM (**Figure 6b**). Upon heating the frozen solutions, tris buffer, at concentrations ≥ 100 mM, exhibited solute crystallization at ~ -50 °C (**Figure 6c**). Irrespective of concentration, eutectic melting at ~ -15 °C, was observed (**Figure 6c**). When the tris HCl was heated, only eutectic melting was observed at ~ -14 °C) (**Figure 6d**). The eutectic melting temperatures of the buffer solutions (-15 to -16°C) were consistently lower than those of pure tris HCl solution (-13 to -14 °C) (**Figure 6c, d**). This depression in the eutectic melting temperature is indicative of the presence of amorphous solute(s) in the system. In the compositions investigated, we have observed that: (i) the

tris base does not crystallize from solution, and (ii) the amorphous tris base partially inhibits the crystallization of tris HCl.

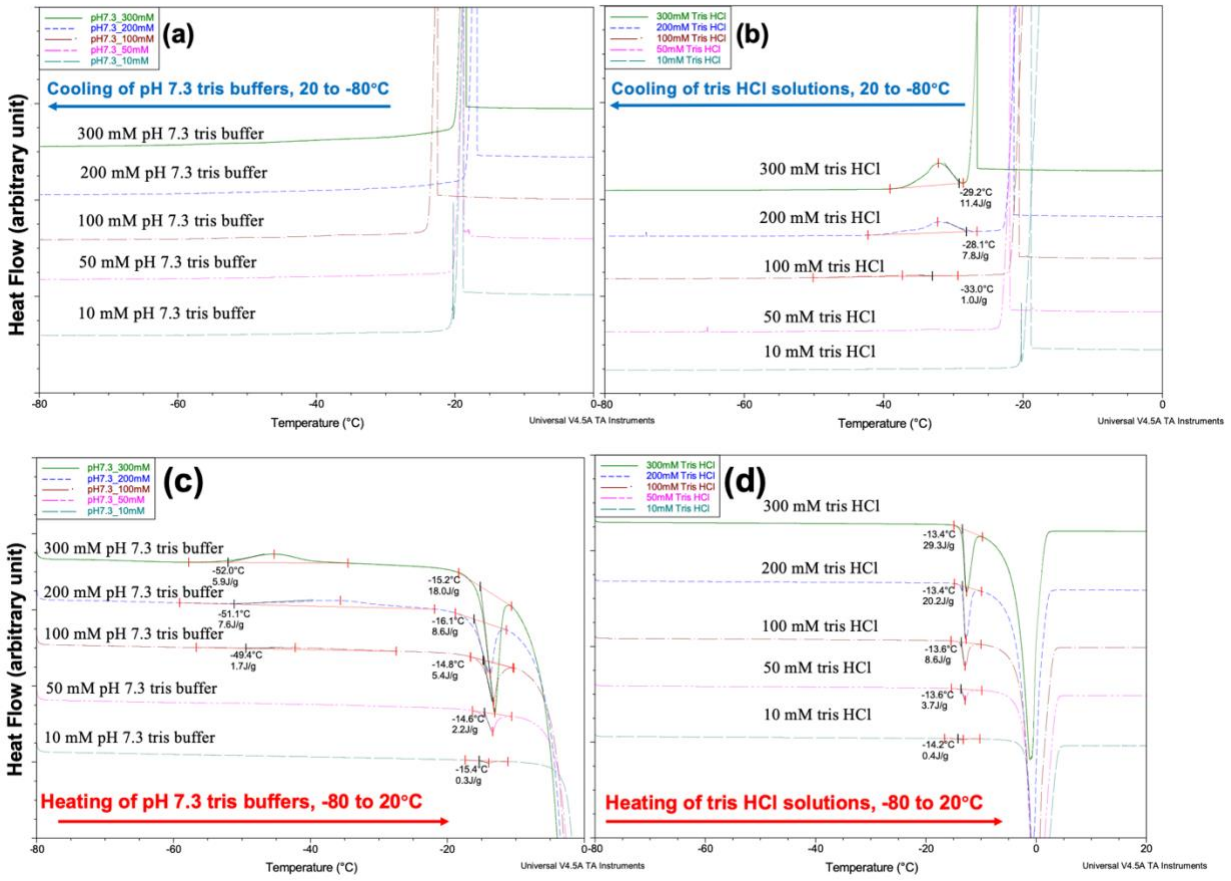

Figure 6. DSC cooling curves of (a) aqueous solutions of pH 7.3* tris buffer and (b) tris HCl. The results of solute concentrations at 500, 300, 200, 100, 50 and 10 mM are shown in green, blue, brown, pink and cyan blue. The solutions were cooled from room temperature (RT) to -80 °C at 1 °C/min. The relevant heating curves of aqueous pH 7.3 tris buffer and tris HCl solutions are shown in panels (c) and (d), respectively. The frozen solutions were heated from -80 to 20 °C at 1 °C/min. *pH measured at RT.

In order to examine this further, the eutectic melting enthalpy obtained as a function of solute concentration was plotted. The eutectic melting enthalpy of both tris HCl and tris buffer increased, almost proportionally, as a function of total solute concentration (**Figure 7**). However, the eutectic melting enthalpy of the buffer solutions was lower than that of pure tris HCl solution. We had

pointed out earlier that, in the buffer solution, 92% of the buffer existed in the ionized form (i.e. tris HCl). The 'theoretical eutectic melting enthalpy' values at each concentration were calculated (grey triangle in **Figure 7**). However, the experimentally observed enthalpy values (green diamond) were consistently lower than the calculated values. The reduction of eutectic melting enthalpy suggests that tris HCl crystallization was inhibited, at least partially, by tris base. As the buffer concentration increased, the inhibitory effect became more pronounced. The eutectic melting values should be viewed with caution. There was an overlap of the eutectic and ice melting endotherms (**Figures 6c** and **6d**). However, we believe that the observed trends are real.

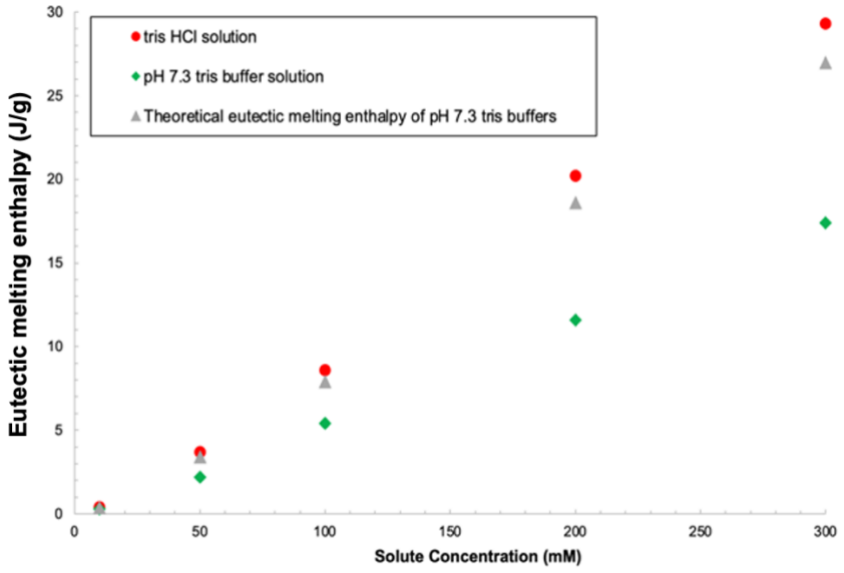

Figure 7. Eutectic melting enthalpy of the frozen aqueous tris HCl (red circle) and tris buffer (pH 7.3) * solutions (green diamond). The gray triangles represent the theoretical melting enthalpy of pH 7.3 buffer solutions. It is based on the assumption that all the tris HCl (92% of the buffer exists in the ionized state at this pH) crystallizes from solution, while the tris base (8%) is retained amorphous. *The pH of the buffer solution was measured at RT.

In an effort to understand this observation, the enthalpy difference (%) between the eutectic melting enthalpy of tris buffer and the 'theoretical value' was plotted against solute concentration in **Figure 8**. As solute concentration increases, the enthalpy difference (%) between the eutectic

melting enthalpy of tris buffer and that of 'theoretical value' generally increases. Thus, the reduction of eutectic melting enthalpy suggests that tris HCl crystallization was inhibited, at least partially, by tris base.

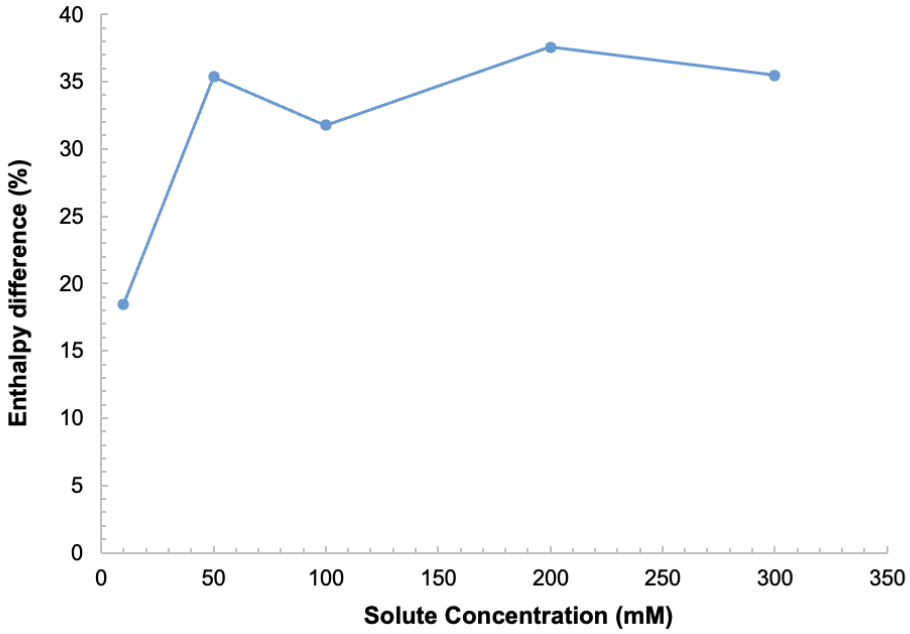

Figure 8. Enthalpy difference (%) between the eutectic melting enthalpy of pH 7.3* buffer and the theoretical value (details in **Figure 7**). It is based on the assumption that all the tris HCl (92% of the buffer exists in the ionized state at this pH) crystallizes from the solution, while the tris base (8%) is retained amorphous. *The pH of the buffer solution was measured at RT.

According to the DSC results, (i) both tris base and tris HCl crystallized during freeze thawing. (ii) Compared with tris base, tris HCl exhibited a higher crystallization propensity. (iii) The crystallization of tris HCl was more pronounced at higher solute concentrations. (iv) As the concentration of tris base increased (i.e., higher pH), there was more pronounced inhibition of tris HCl crystallization. In other words, tris base exhibited a concentration dependent inhibition of tris HCl crystallization.

Synchrotron X-ray diffractometry (SXRD)

The phase behavior of tris buffer solutions at subambient conditions was further investigated by X-ray diffractometry using synchrotron radiation. The solutions were first cooled to -40 °C and then heated to 5 °C. The diffraction patterns are shown in **Figure 9 - 11, S2- 6**.

When a solution of tris HCl (100 mM) was cooled, solute crystallization was evident at -40 °C (**Figure 9**). When the solutions were heated, there was further solute crystallization at -35 °C, evident from the increase in peak intensities. At -15 °C, the diffraction peak attributed to crystalline tris HCl disappeared, which was in excellent agreement with the eutectic melting temperature (-14 °C) measured using DSC (**Figure 6d**).

Under these experimental conditions, the hexagonal (I_h) and cubic (I_c) forms of ice are expected[20]. However, the crystal forms in the current study were highly variable and cannot be attributed to either I_h or I_c forms of ice. In the current cooling setup, the inhomogeneous cooling, and the pronounced supercooling are likely responsible for the run-to-run variability in the crystal forms of ice [20]. Similar observations were also revealed in studies from our group (Li et. al., unpublished work). However, ice phase transformation was not detected during a single freeze thawing cycle, which facilitated the unambiguous characterization of solute crystallization if any.

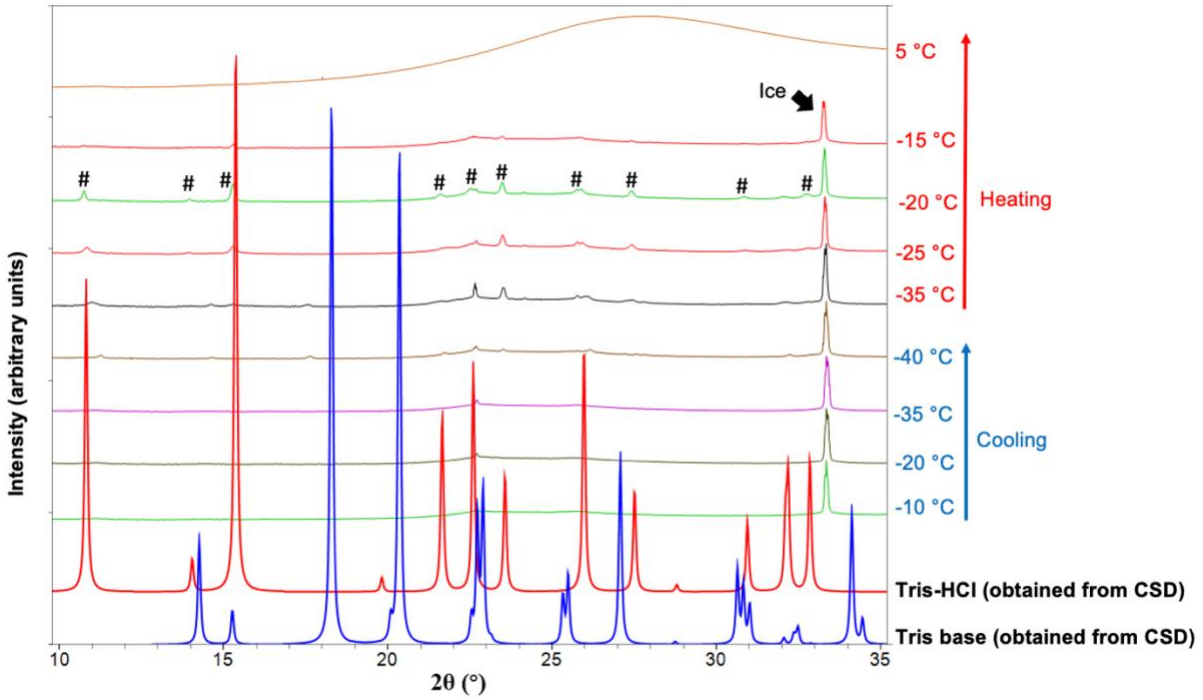

Figure 9. SXRD patterns of tris HCl (100 mM) solution during freezing and heating. The solution was cooled from room temperature to -40 °C, held for 15 min, and then heated to 5 °C. The crystalline peaks of tris HCl are highlighted with "#". The results collected using synchrotron radiation (0.45171 Å) were converted to Cu Kα radiation (1.54 Å) to facilitate ready comparison with published data. The reference X-ray patterns of tris base and tris HCl were obtained from the Cambridge Structural Database (Refcode: THXMAM15 and TRISHC10).

During the cooling of 100 mM tris base solution, the crystalline phase of tris base was not observed (**Figure 10**). Upon heating, tris base crystallized at -25 °C, at a temperature higher than in the DSC (-41 °C). This discrepancy could be attributed to both differences in sample geometry and the experimental conditions. The diffraction peaks of tris base completely disappeared at -5 °C, which is in excellent agreement with the eutectic temperature of -6 °C determined by DSC (**Figure 4c**).

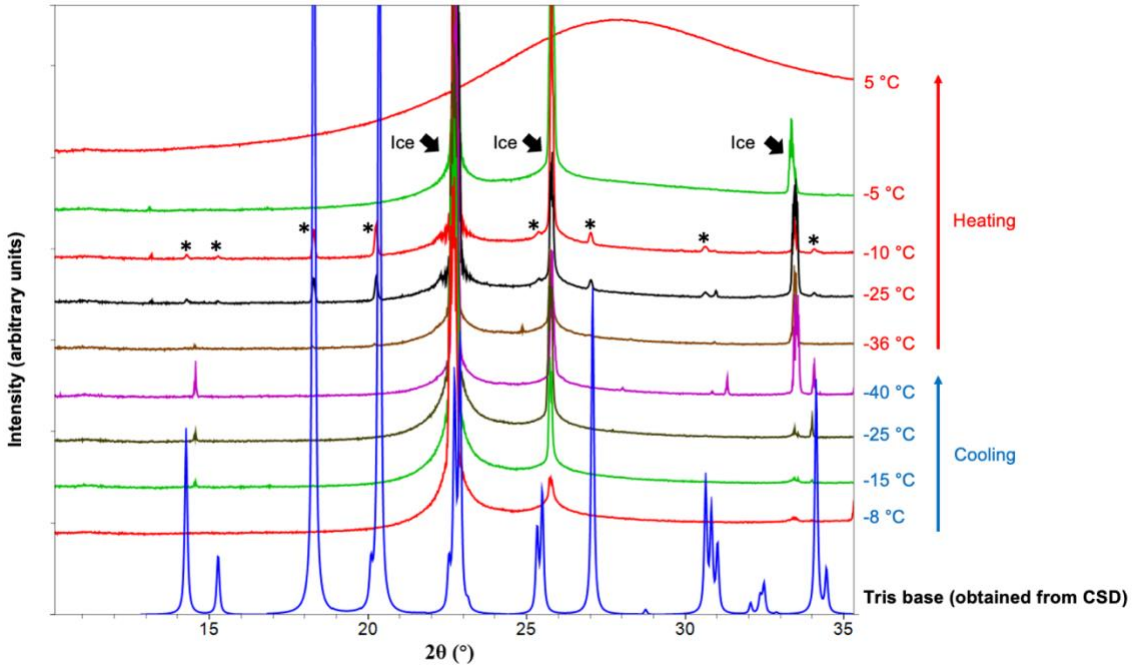

Figure 10. SXRD patterns of 100 mM tris base solution during freezing and heating. The solution was cooled from room temperature to -40 °C, held for 15 min, and heated to 5 °C. The crystalline phase of tris base was highlighted with "*". The results collected using synchrotron radiation (0.45171 Å) were converted to Cu Kα radiation (1.54 Å) to facilitate ready comparison with published data. The reference X-ray pattern of tris base was obtained from the Cambridge Structural Database (Refcode: THXMAM15).

When the tris buffer solution (100 mM, initial pH 7.3) was cooled, there was no solute crystallization. On heating, crystallization of tris HCl was observed at -32 °C (**Figure 11**). In our DSC studies, there was no evidence of solute crystallization (**Figure 5b**). While the tris HCl peaks were observed up to -12 °C, they disappeared at -10 °C (eutectic melting). At a lower buffer concentration (10 mM), in the DSC, solute crystallization was revealed by the eutectic melting (**Figure 6d**). In SXRD, peaks attributable to tris HCl were not observed (**Figure S2**). The absence of solute crystallization during the freeze thawing of buffer solutions with initial pH values of 8.0 and 8.8 agreed with the DSC results (**Figure 5; SXRD Figure S3 - 6**).

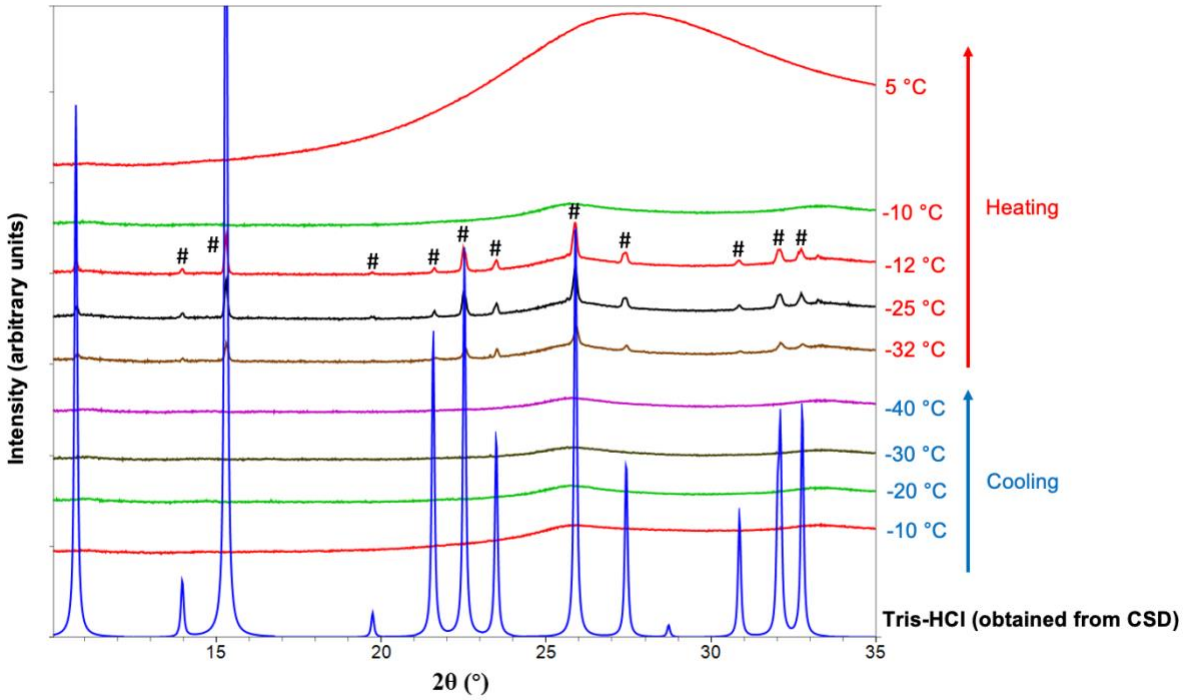

Figure 11. Synchrotron XRD of 100 mM tris HCl buffer (pH 7.3)* during freezing and heating. The solution was cooled from room temperature to -40 °C, held for 15 min, and heated to 5 °C. The crystalline phase of tris HCl was highlighted with "#". The results collected using synchrotron radiation (0.45171 Å) were converted to Cu Kα radiation (1.54 Å) to facilitate ready comparison with published data. The reference X-ray pattern of tris HCl was obtained from the Cambridge Structural Database (Refcode: TRISHC10). * pH measured at room temperature.

Based on the DSC and SXRD results, at subambient conditions, tris HCl has a substantially higher crystallization propensity than tris base. Its crystallization, which was often observed during heating, is expected to cause a pronounced increase in solution pH value. The positive pH shift can be further exacerbated with the increase in the buffer pK_a. Therefore, our next step was to measure the "pH" of frozen tris solutions during heating, at predetermined temperatures (-40, -30, and -20 °C).

Low temperature pH measurement

In order to measure the pH of frozen tris solutions, cresol red (CR) was added as the pH indicator. The three forms of the dye, H_2CR, $H(CR)^-$ and $(CR)^{2-}$, exhibit absorbance maxima at 518, 434 and 573 nm respectively. However, since the pH of buffer solutions ranged from 7.3 to 8.5, only the absorbance peaks attributed to $H(CR)^-$ and $(CR)^{2-}$ can be detected (within ± 2 units of the second pK_a (8.2) of the dye). The peak positions of the above two forms of CR were not substantially influenced by temperature (**Table S11**). As the ratio of $H(CR)^-$ and $(CR)^{2-}$ decreased, the pH of the buffer solution increased (**Figure 12**). Such a change in the UV spectrum can be used to quantitively evaluate the potential pH (or acidity function, H_x) increase as a result of either tris HCl crystallization or increase in the pK_a of the buffer systems during freeze thawing.

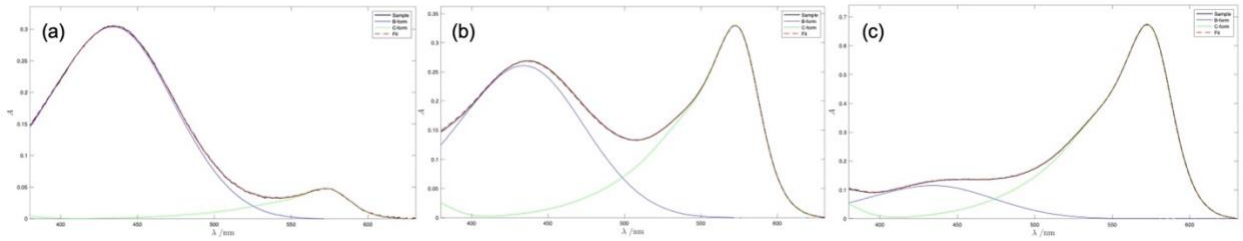

Figure 12. Fitting of UV-Vis spectra of tris buffer (pH = 7.3, 7.9 and 8.5)* containing 0.055 mg cresol red (CR). The reference spectra of $H(CR)^-$ and $(CR)^{2-}$ (blue and green lines, respectively) were obtained from the absorbance measurements of the solutions of pH 4.5 and 11.5 containing the same concentration of the dye. The spectra of the sample solutions are shown in black. The fitted curve is shown as red dashed line which is the sum of the two reference spectra. The fitted and the experimental data are in excellent agreement. The spectra of tris solutions at pH 7.3, 7.9 and 8.5 (at RT) are shown in panels (a), (b) and (c) respectively. *pH measured at room temperature.

The measured H_x values of buffer solutions are summarized in **Table 2**. The pH_0 values of buffers obtained using UV-Vis spectra and acidity function match the results obtained by using a pH meter. Compared with pH_0, all the frozen buffer solutions exhibited a positive pH shift. For the solution with pH_0 of 7.3 and 7.5, the increase in H_x value was more pronounced at lower temperatures. A

similar effect was also observed in pH 7.9 buffer solution (100 mM). However, for solutions with a higher initial pH (pH_0 8.5), the pH increases in the frozen solutions resulted in the absence of the $H(CR)^-$ peak in their UV spectra. This means the H_x value possibly exceeded the detection limit of the dye (H_x >10.2). Based on the SXRD results, the crystallization of tris HCl was initiated upon cooling to -32 °C and continued during heating until its eutectic melting at -10 °C (**Figure 9**). We will begin the discussion with the assumption that the temperature dependence of the buffer pK_a was not playing a major role in the pH shift. In that case, the progressive crystallization of tris HCl is expected to cause a continuous increase in the pH during heating. The pH increase (expressed as $H_x - pH_0$) as a function of heating temperature is evident from **Figure 13**.

Table 2. Initial pH (pH_0) of tris buffer solutions at RT and their acidity function (H_x) at different temperatures during heating of the frozen solution.

Concentration	pH_0	H_x (at -40 °C)	H_x (frozen solution heated to -30°C)	H_x (frozen solution heated to -20 °C)
10 mM	7.3	9.0	8.9	8.3
100 mM	7.5	9.2	8.9	8.4
10 mM	7.9	9.2	8.9	8.6
100 mM	7.9	9.5	9.0	8.8
10 mM	8.5	9.5	>10.2*	8.9
100 mM	8.5	>10.2*	9.3	>10.2*

*Outside the detection limit of the dye

Figure 13 summarizes the pK_a changes and pH shift ($H_x - pH_0$) of tris buffer solutions. Surprisingly, the positive pH shift was more pronounced at lower temperatures, suggesting that the "additional" buffer salt crystallization during heating did not have a pronounced effect. In addition, the buffer concentration and pH_0 did not have a pronounced effect on the pH shift (**Figure 13a** and **b**). As we discussed earlier, the pK_a of tris buffer system is highly temperature dependent

(theoretically +0.41 unit per 10 °C decrease in temperature). The change in pK_a, may mask the effect of buffer salt crystallization. In the current study of buffers with pH_0 7.3, 7.5, and 7.9, the increase in H_x is ~ 0.3 to 0.4 unit per 10 °C temperature decrease, possibly indicating that the positive pH shift of tris buffer at subambient conditions is attributable to increasing pK_a rather than tris HCl crystallization. Trend lines were labeled in **Figure 13** to describe the approximately linear relationship between the pH shift and temperature of both buffers and the pK_a values of the buffer.

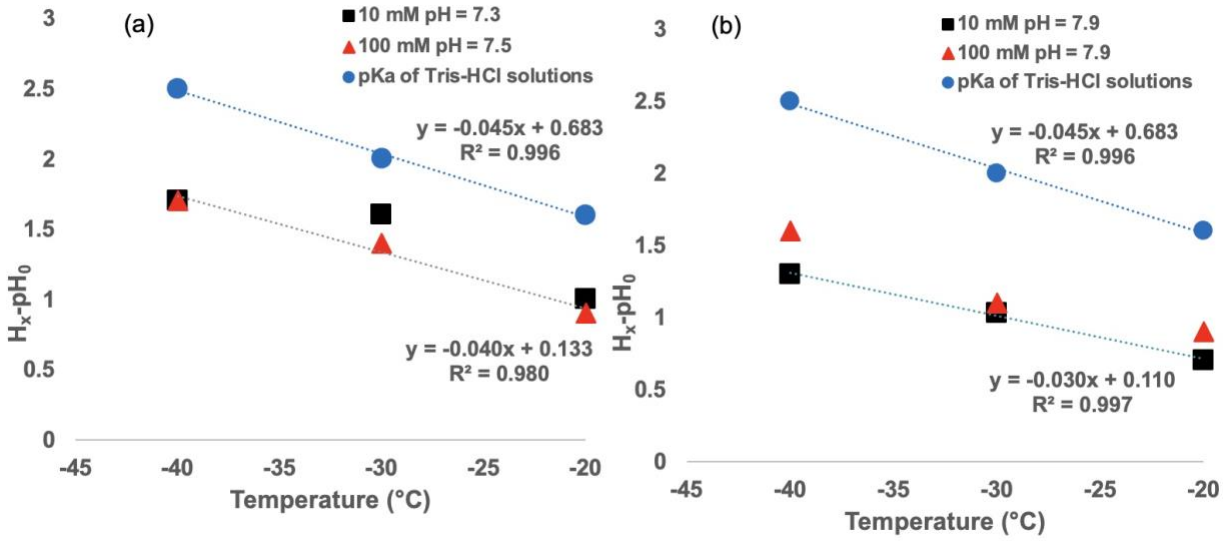

Figure 13. pH shift (H_x – pH_0) and pK_a (blue circle) at -40, -30 and -20 °C during heating. The results of 10 mM pH 7.3* (black square) and 100 mM pH 7.5* (red triangle) tris buffers are shown in panel (a). Panel (b) reveals the pH shift of 10 mM (black square) and 100 mM (red triangle) pH 7.9* tris solutions. Linear trendline of pK_a (blue dash line), 100 mM pH 7.5* (red dash line), and 10 mM pH 7.9* (black dash line) tris buffers were shown with equation and R^2. *Initial pH at RT.

Effect of annealing on the solute crystallization in tris buffers

Although tris HCl crystallization was not the key factor responsible for the pH shift during freeze thawing, the buffer salt crystallization may occur during isothermal frozen storage (annealing), resulting in an additional pH shift. Thus, an annealing step (-20 °C, 8 h) was conducted to induce buffer salt crystallization. The annealed frozen solutions were cooled back to -50 °C, and the second heating curves are shown in **Figures 14** and **S7, 8**. In solution buffered to pH_0 8.0 (both 10 and 100 mM), annealing resulted in the appearance of an endotherm at ~ -14 °C, which is attributed to the eutectic melting of crystalline tris HCl (**Figures 14a** and **14b**). Thus, annealing caused the crystallization of tris HCl. In solution buffered to pH_0 7.3 (10 and 100 mM), the eutectic melting enthalpy was not substantially changed after annealing, indicating that the crystallization of tris HCl was possibly complete during the first freeze thaw cycle (**Figures 13c and 13d**). No additional thermal event (e.g., eutectic melting) was observed in the second DSC heating curve of solutions with pH_0 of 8.8 (**Figure S7, S8**). The above results pointed out that tris HCl had the potential to crystallize during annealing while tris base was highly resistant to crystallization.

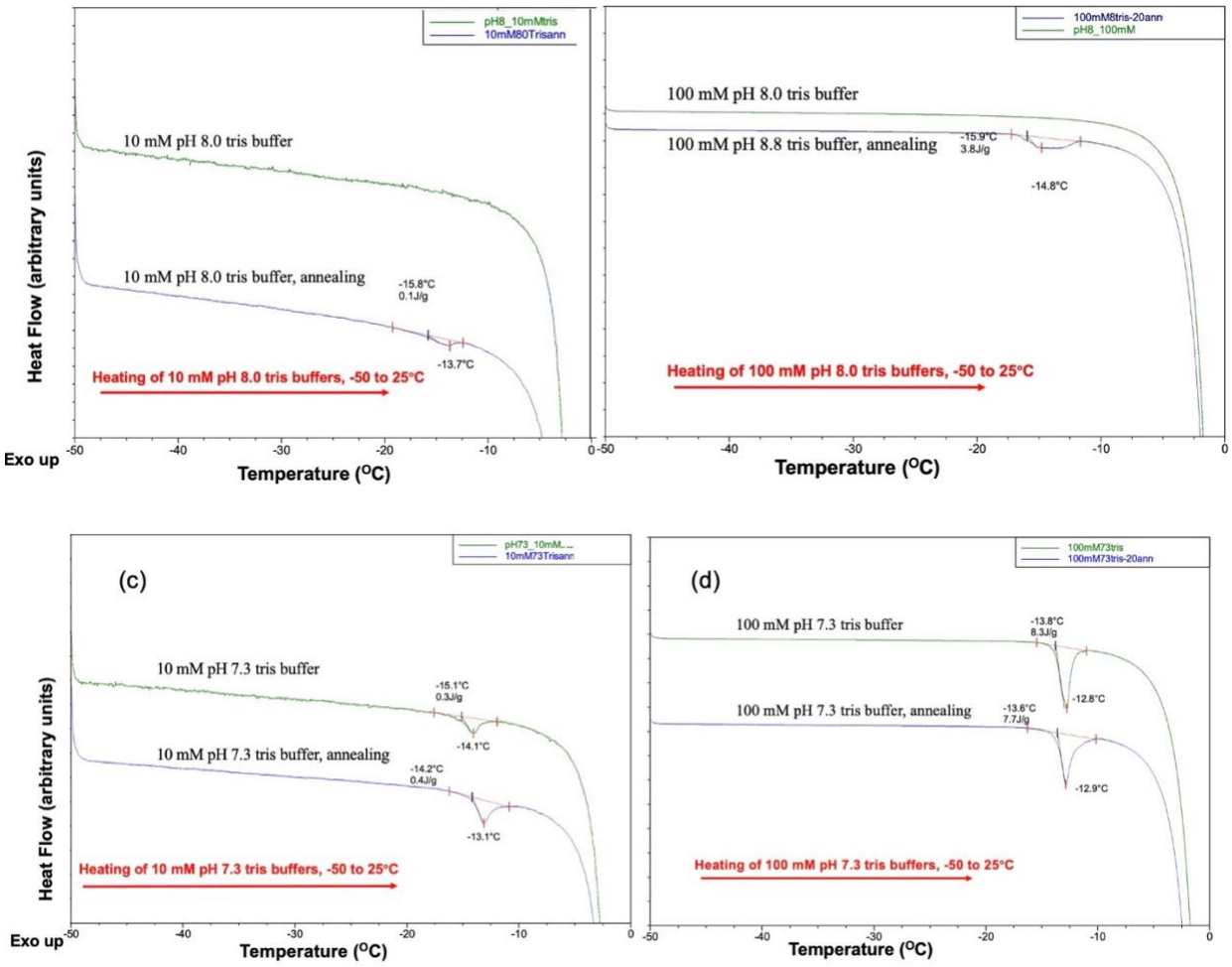

Figure 14. DSC heating curves of (a) 10 mM pH 8.0* tris solution, (b) 100 mM pH 8.0* tris solution, (c) 10 mM pH 7.3* tris solution, and (d) 100 mM of pH 7.3* tris solution. Green curve - heating from -50 to 20 °C without annealing; blue curve - heating from -50 to 20 °C after annealing at -20 °C for 8 hours. * pH measured at room temperature.

CONCLUSION

According to the DSC results, (i) both tris base and tris HCl crystallized during freeze thawing. (ii) Compared with tris base, tris HCl exhibited a higher crystallization propensity. (iii) The crystallization of tris HCl was more pronounced at higher solute concentrations. (iv) As the concentration of tris base increased (i.e., higher pH), there was more pronounced inhibition of tris HCl crystallization. In other words, tris base exhibited a concentration dependent inhibition of tris HCl crystallization. Cresol red (CR) was added as the pH indicator to measure the pH of frozen tris solutions. The positive pH shift was more substantial at lower temperatures, indicating that the buffer salt crystallization during heating was not responsible for pH change. Besides, buffer concentration and pH_0 (when $pH_0 \leq 7.9$) did not influence the trend of pH shifts as heating temperature increased (**Figures 13a and 13b**). As we discussed earlier, the pK_a of tris buffer system is highly temperature dependent (theoretically + 0.41 unit per 10 °C decrease), which may far exceed the effect of buffer salt crystallization. In the current study of buffers with pH_0 7.3, 7.5, and 7.9, the increase in H_x is ~ 0.3 to 0.4 unit per 10 °C decrease, possibly indicating that the positive pH shift of tris buffer at subambient conditions is attributable to increasing pK_a rather than tris HCl crystallization. Formulators should be aware of the positive pH shift of tris buffer at subambient conditions since it may influence protein stability.

APPENDIX

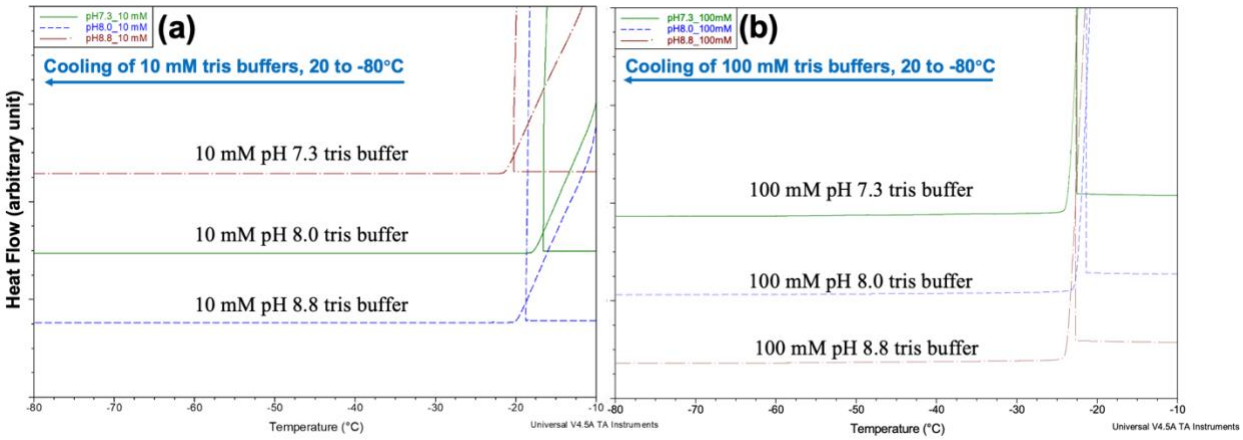

Figure S1. DSC cooling curves of (a) 10 and (b) 100 mM tris buffer solutions. The pH values of the buffer solutions are 7.3*, 8.0* and 8.8* (green, blue, and brown lines). The solutions were cooled from 5 to -80 °C at 1°C/min. *pH measured at room temperature.

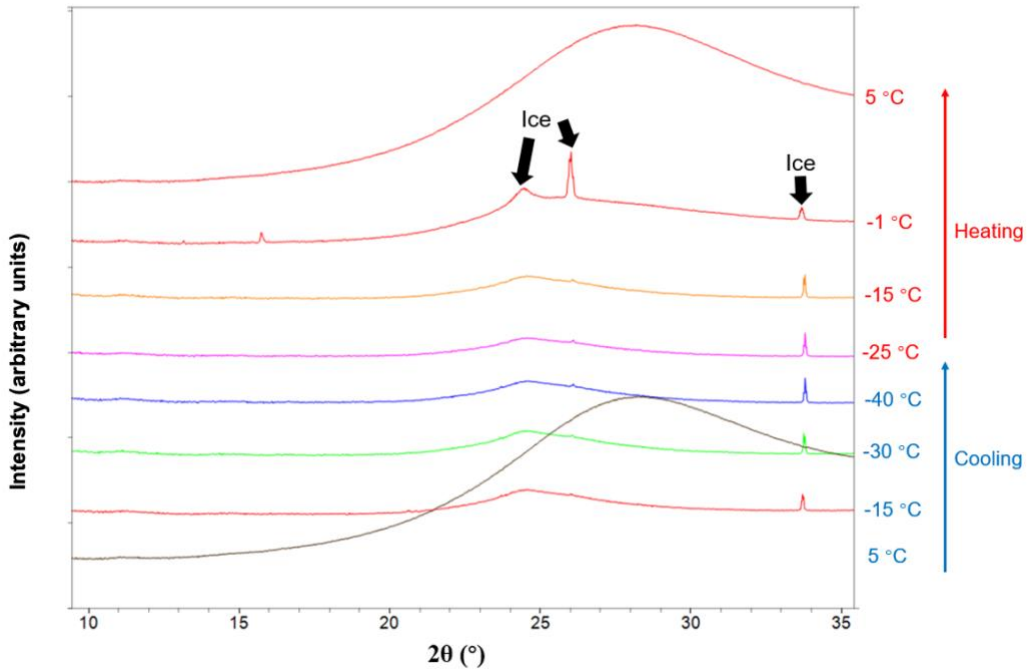

Figure S2. Synchrotron XRD of 10 mM tris HCl buffer (pH 7.3*) during freezing and heating. The solution was cooled from room temperature to -40 °C, held for 15 min, and heated to 5 °C. The results collected using synchrotron radiation (0.45171 Å) were converted to Cu Kα radiation (1.54 Å) to facilitate ready comparison with published data. *pH measured at room temperature.

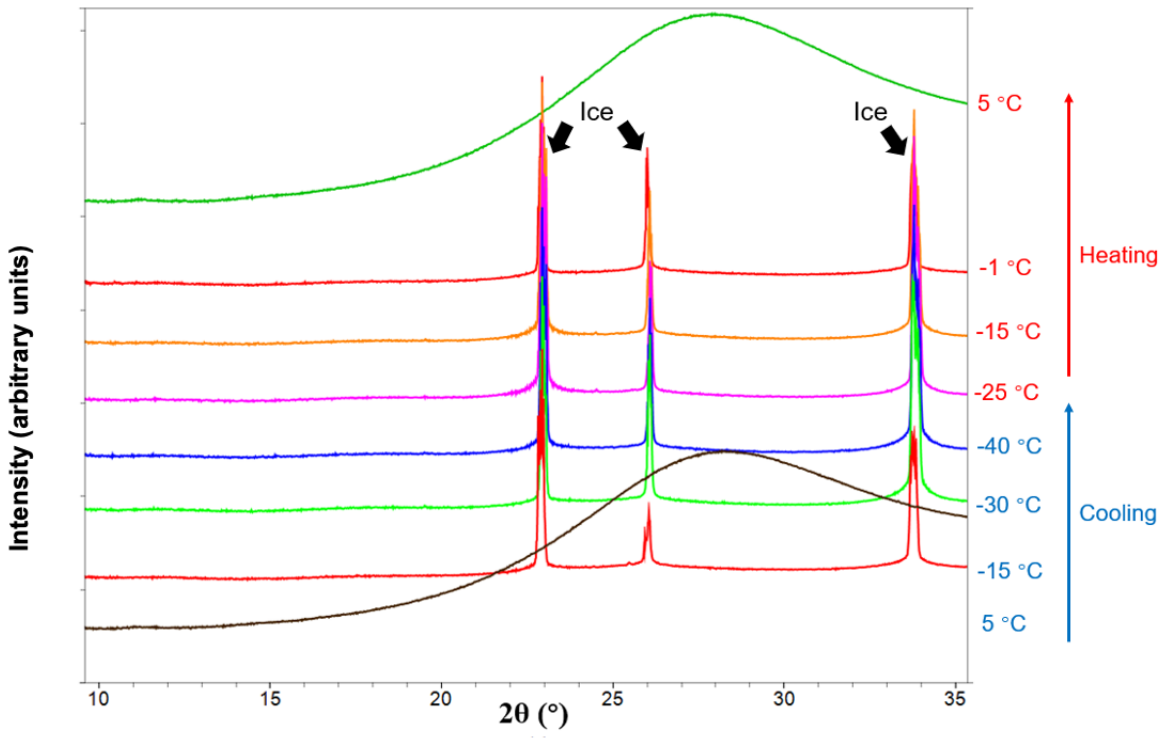

Figure S3. Synchrotron XRD of 10 mM tris HCl buffer with pH 8.0* during freezing and heating. The solution was cooled from room temperature to -40 °C, held for 15 min, and heated to 5 °C. The results collected using synchrotron radiation (0.45171 Å) were converted to Cu Kα radiation (1.54 Å) to facilitate ready comparison with published data. *pH measured at room temperature.

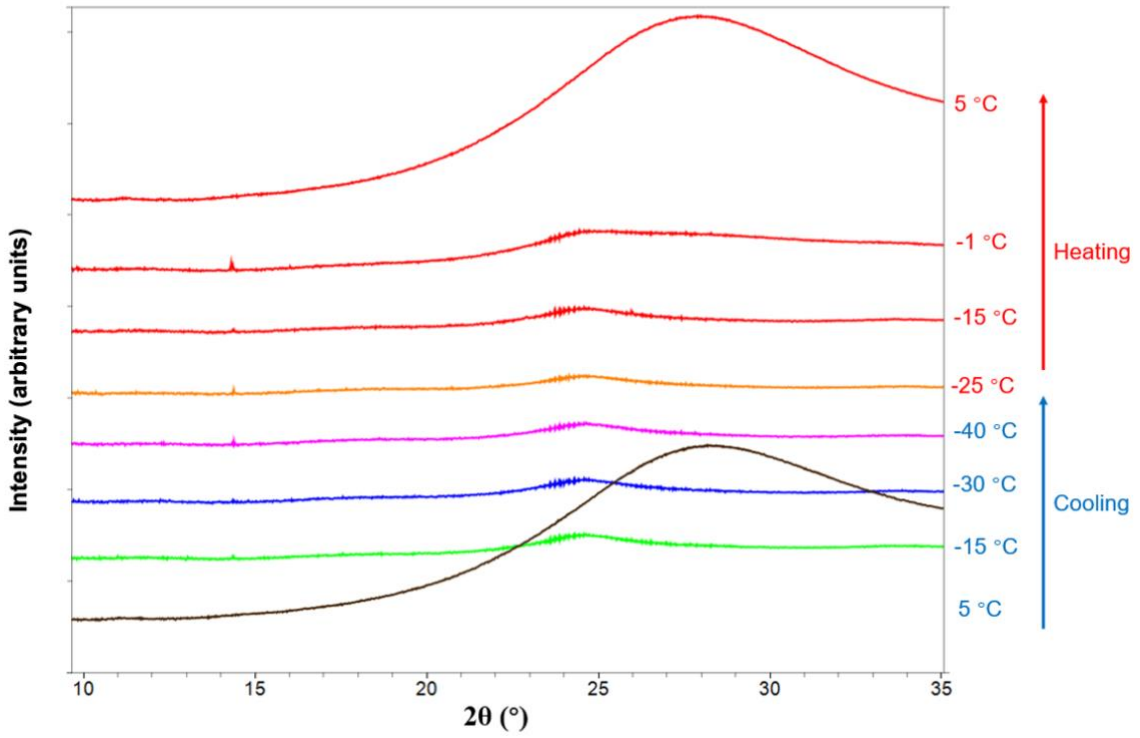

Figure S4. Synchrotron XRD of 100 mM tris HCl buffer with pH 8.0* during freezing and heating. The solution was cooled from room temperature to -40 °C, held for 15 min, and heated to 5 °C. The results collected using synchrotron radiation (0.45171 Å) were converted to Cu Kα radiation (1.54 Å) to facilitate ready comparison with published data. *pH measured at room temperature.

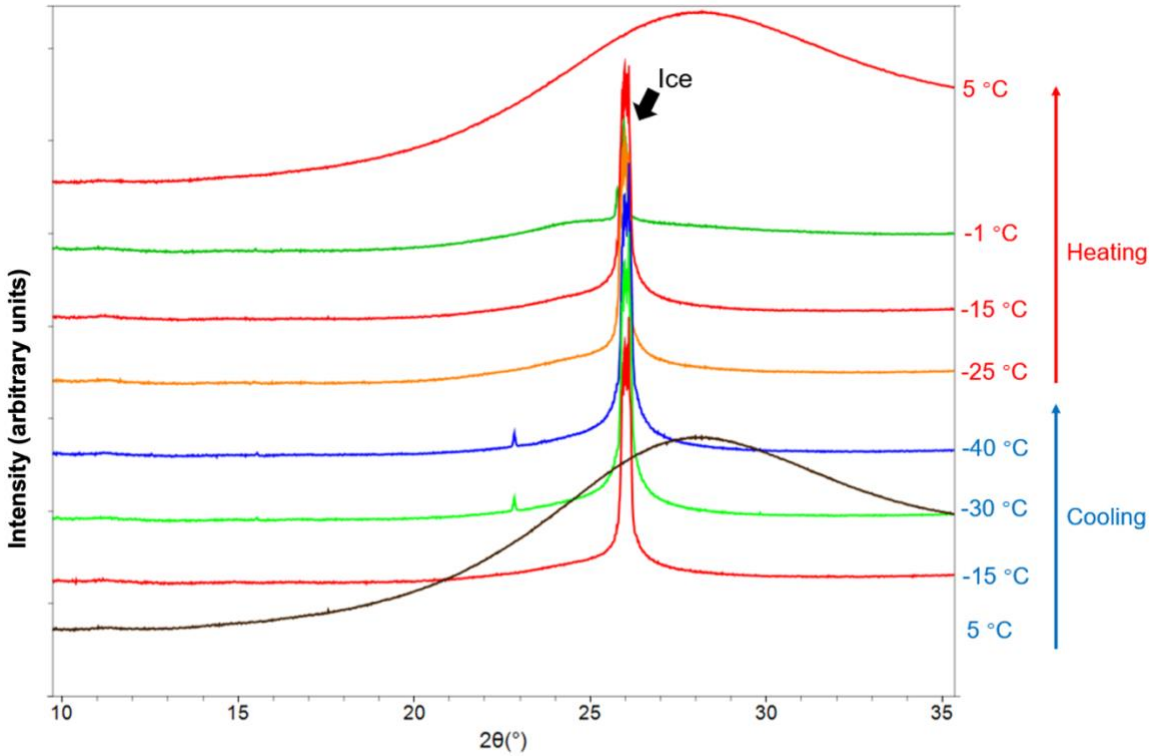

Figure S5. Synchrotron XRD of 10 mM tris HCl buffer (pH 8.8*) during freezing and heating. The solution was cooled from room temperature to -40 °C, held for 15 min, and heated to 5 °C. The results collected using synchrotron radiation (0.45171 Å) were converted to Cu Kα radiation (1.54 Å) to facilitate ready comparison with published data. *pH measured at room temperature.

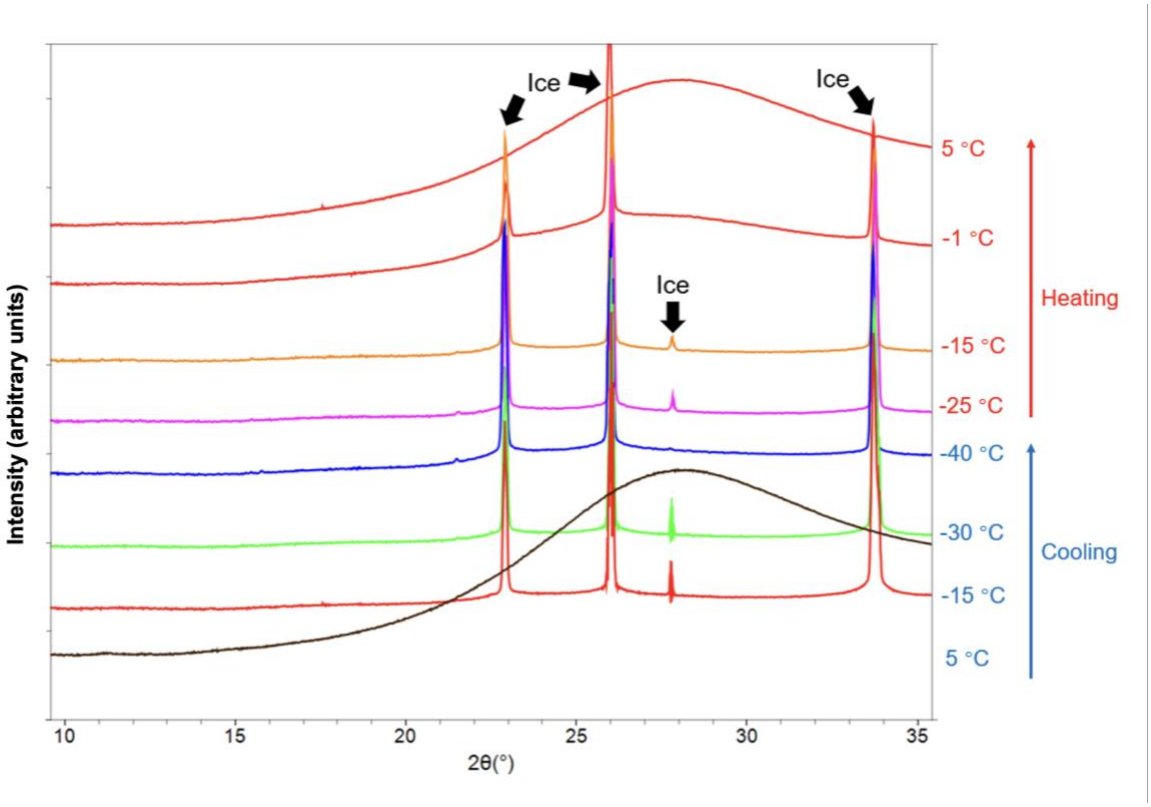

Figure S6. Synchrotron XRD of 100 mM tris HCl buffer (pH 8.8*) during freezing and heating. The solution was cooled from room temperature to -40 °C, held for 15 min, and heated to 5 °C. The results collected using synchrotron radiation (0.45171 Å) were converted to Cu Kα radiation (1.54 Å) to facilitate ready comparison with published data. *pH measured at room temperature.

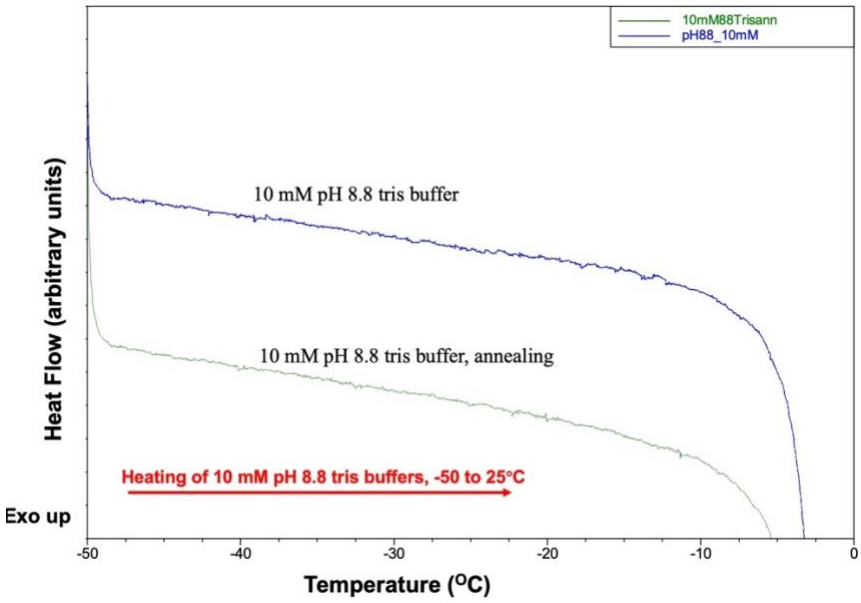

Figure S7. DSC heating curves of 10 mM of tris HCl buffer (pH 8.8*) without annealing and after annealing at -20 °C for 8 hours (blue and green, respectively). The temperature range is from -50 to 25 °C and the heating rate was 1°C/min. * pH measured at room temperature. The solutions were initially cooled from 5 to -50 °C at 1 °C/min.

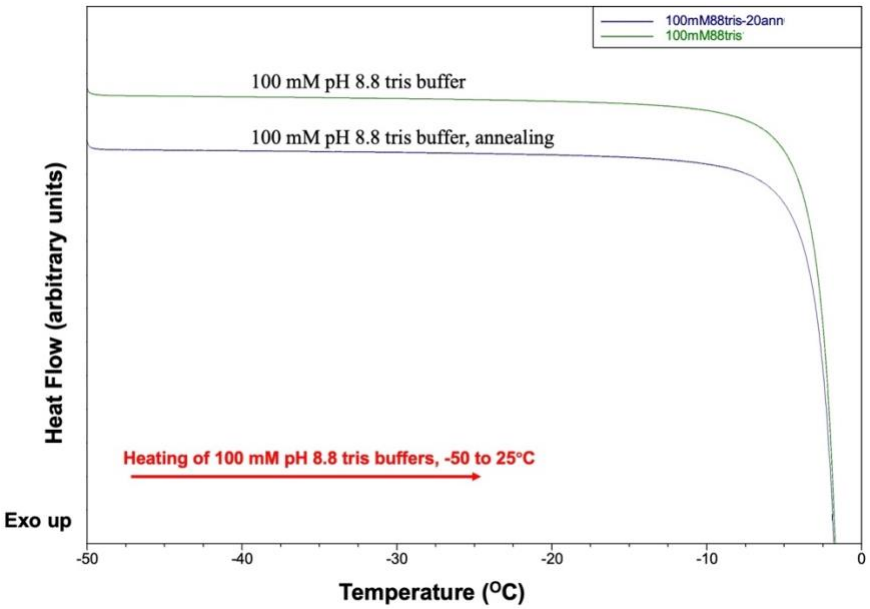

Figure S8. DSC heating curves of 100 mM tris HCl buffer (pH 8.8*) without annealing (green) and after annealing at -20 °C for 8 hours (blue). The temperature range is from -50 to 20 °C with a heating rate of 1°C/min. The solutions were initially cooled from 5 to -50 °C at 1 °C/min. * pH measured at room temperature.

Script S9: H_x value calculation based on the ratio of protonated and deprotonated forms of CR.

```
c = lsqnonneg ([ind_form1, ind_form2], sample_spectrum);

Hx= pKa_ind+log10(c(2)/ c(1));
```

Absorbances of protonated (*ind_form1*), deprotonated form (*ind_form2*) of CR, and sample (*sample_spectrum*) are vector inputs. Ratio of *c(1)* and *c(2)* showed the relative abundance of protonated and deprotonated forms of CR.

Table S10. Peak positions of $H(CR)^-$ (B form) and $(CR)^{2-}$ (C form) under subambient temperatures.

CR form	Peak position (nm) Solution (RT)	-20 °C	-30 °C	-40 °C
$H(CR)^-$	434	443	436	443
$(CR)^{2-}$	572	575	574	575

REFERENCES

1. Kulkarni, S. S.; Patel, S. M.; Suryanarayanan, R.; Rinella, J. V.; Bogner, R. H. Key Factors Governing the Reconstitution Time of High Concentration Lyophilized Protein Formulations. *European Journal of Pharmaceutics and Biopharmaceutics* **2021**, 165, 361–373.

2. Gervasi, V.; Dall Agnol, R.; Cullen, S.; McCoy, T.; Vucen, S.; Crean, A. Parenteral Protein Formulations: An Overview of Approved Products Within the European Union. *European Journal of Pharmaceutics and Biopharmaceutics* **2018**, 131, 8–24.

3. Reinsch, H.; Spadiut, O.; Heidingsfelder, J.; Herwig, C. Examining the Freezing Process of an Intermediate Bulk Containing an Industrially Relevant Protein. *Enzyme and Microbial Technology* **2015**, 71, 13–19.

4. Thakral, S.; Sonje, J.; Munjal, B.; Suryanarayanan, R. Stabilizers and Their Interaction with Formulation Components in Frozen and Freeze-Dried Protein Formulations. *Advanced Drug Delivery Reviews* **2021**, 173, 1–19.

5. Bristol-Mysers Squibb. YERVOY® (ipilimumab). https://www.yervoy.com/ (accessed May 27, 2023).

6. Partner Therapeutics. LEUKINE® sargamostim. https://www.leukine.com/ (accessed May 27, 2023).

7. Zbacnik, T. J.; Holcomb, R. E.; Katayama, D. S.; Murphy, B. M.; Payne, R. W.; Coccaro, R. C.; Evans, G. J.; Matsuura, J. E.; Henry, C. S.; Manning, M. C. Role of Buffers in Protein Formulations. *Journal of Pharmaceutical Sciences* **2017**, 106 (3), 713–733.

8. Madmon, M.; Shamai Yamin, T.; Pitel, S.; Belay, C.; Segula, Y.; Toister, E.; Hindi, A.; Cherry, L.; Ophir, Y.; Zichel, R.; Mimran, A.; Diamant, E.; Weissberg, A. Development and Validation of an Innovative Analytical Approach for the Quantitation of Tris(Hydroxymethyl)Aminomethane (TRIS) in Pharmaceutical Formulations by Liquid Chromatography Tandem Mass Spectrometry. *Molecules (Basel, Switzerland)* **2022**, *28* (1), 73.

9. Tris Base, ULTROL® Grade. https://www.sigmaaldrich.com/US/en/product/mm/648311(accessed May 27, 2023).

10. Goldberg, R. N.; Kishore, N.; Lennen, R. M. Thermodynamic Quantities for the Ionization Reactions of Buffers. *Journal of Physical and Chemical Reference Data* **2002**, *31* (2), 231–370.

11. Samuelsen, L.; Holm, R.; Lathuile, A.; Schönbeck, C. Buffer Solutions in Drug Formulation and Processing: How pKa Values Depend on Temperature, Pressure and Ionic Strength. *International Journal of Pharmaceutics* **2019**, *560*, 357–364.

12. Kolhe, P.; Amend, E.; K. Singh, S. Impact of Freezing on pH of Buffered Solutions and Consequences for Monoclonal Antibody Aggregation. *Biotechnology Progress* **2010**, 26 (3), 727–733.

13. Thorat, A. A.; Munjal, B.; Geders, T. W.; Suryanarayanan, R. Freezing-Induced Protein Aggregation - Role of pH Shift and Potential Mitigation Strategies. *Journal of Controlled Release* **2020**, *323*, 591–599.

14. Chang, B. S.; Randall, C. S. Use of Subambient Thermal Analysis to Optimize Protein Lyophilization. *Cryobiology* **1992**, *29* (5), 632–656.National Library of Medicine.

15. Cresol red. https://pubchem.ncbi.nlm.nih.gov/compound/Cresol-red#:~:text=Cresol%20red%20is%20a%20member,and%20a%20two%2Dcolour%20indicator (accessed May 27, 2023)

16. Vetráková, Ľubica; Vykoukal, V.; Heger, D. Comparing the Acidities of Aqueous, Frozen, and Freeze-Dried Phosphate Buffers: Is There a "pH Memory" Effect? *International Journal of Pharmaceutics* **2017**, *530* (1-2), 316–325.

17. Heger, D.; Klánová, J.; Klán, P. Enhanced Protonation of Cresol Red in Acidic Aqueous Solutions Caused by Freezing. *The Journal of Physical Chemistry. B* **2006**, *110* (3), 1277–1287.

18. Sonje, J.; Thakral, S.; Suryanarayanan, R., t-Butanol Enables Dual Functionality of Mannitol: A Cryoprotectant in Frozen Systems and Bulking Agent in Freeze-Dried Formulations. *Molecular Pharmceutics* **2020**, 17 (8), 3075-3086.

19. Hammett, L. P.; Deyrup, A. J. A Series of Simple Basic Indicators. I. The Acidity Functions of Mixtures of Sulfuric and Perchloric Acids with Water. *Journal of the American Chemical Society* **1932**, 54 (7), 2721–2739.

20. Malkin, T. L.; Murray, B. J.; Brukhno, A. v.; Anwar, J.; Salzmann, C. G. Structure of Ice Crystallized from Supercooled Water. *Proceedings of the National Academy of Sciences* **2012**, *109* (4), 1041–1045.